Macromolecules
ARTICLE

Macromolecules **2010**, *43*, 9191–9197 **9191**
DOI: 10.1021/ma1020402

Prediction of Bulk Density and Molecular Packing in Model Dendrimers with Different Chain Stiffness

Paola Carbone*,† and Leo Lue‡

†*School of Chemical Engineering and Analytical Science, The University of Manchester, Oxford Road, M13 9PL, United Kingdom, and* ‡*Department of Chemical and Process Engineering, University of Strathclyde, James Weir Building, 75 Montrose Street, Glasgow G1 1XJ, United Kingdom*

Received September 2, 2010; Revised Manuscript Received October 1, 2010

ABSTRACT: By means of molecular dynamics simulations of model dendrimers, we analyze the dependence of the bulk density and molecular packing on the dendrimer molecular weight and intrinsic stiffness. We find that the density is consistently higher in flexible dendrimers than in the rigid ones with a large bending angle. The density values change slightly within the first two generations to reach a plateau. We interpret these results in terms of free volume, showing that the enhanced accessible free volume that characterizes the end-dendron monomers is counterbalanced by the higher number of internal monomers, leading to a constant bulk density for generations larger than three. The added stiffness affects the geometrical properties and the molecular rearrangement of the bulk, reducing the short-range local order and the packing efficiency favoring the dendrimer interpenetration. Our prediction for the bulk density matches and rationalizes experimental and previous all-atom simulation results.

Introduction

Dendrimers are hyperbranched macromolecules characterized by a very high degree of symmetry in their topology. They have a multifunctional core from which relatively short chains (called branches or dendrons) emanate.[1] Because of their striking topology, they are considered a special class of macromolecules, and in fact their properties differ quite remarkably from other corresponding polymers.[2,3] In order to use dendrimers as materials,[4−6] accurate knowledge of their properties in the bulk phase is necessary. In particular, the study of the dependence of the glass transition temperature,[7] viscosity,[8,9] and molecular shape and organization[10,11] on dendrimer generation and topology is vital to optimize their applications. Several experimental and theoretical investigations have addressed different aspects of the thermodynamic[2,12−15] and rheological behavior[11,16,17] of dendrimer melts, but, although all the properties mentioned above depend on the value of the bulk density, a systematic study of its dependence on dendrimer molecular weight or chemical composition is still lacking. In fact, while for linear polymers the relation between glass transition temperature, bulk density, and free-volume is well-known,[18,19] for dendritic molecules this relation has not been clearly established yet.[7,20] One of the main problem seems to be the difficulty to generalize the results to any type of dendrimer, irrespective of its chemical constitution. Indeed, dendrimers of the same generation can show either a compact and spherical shape (filled core conformation) or a more open disk-like shape (hollow-core conformation)[21] depending on the type of monomers used. It is then possible to tune the properties of the final molecule at the first stage of the synthesis, choosing the correct monomer for the target application. The structure and properties of dendrimers are, in fact, not only determined by the monomer chemical composition (polarity, acidity, etc.) but also by the nature of the covalent bonds connecting the monomers. Indeed, due to their constrained topology, in dendrimers the presence of rigid monomers, such as phenylene, leads to a reduced number of allowed conformations and, in turn, can change the entire global shape of the molecule.[22] A similar effect has been also reported for linear polymers where the glass transition temperature can be modulated by varying distribution and concentration of bulky rigid units.[23]

Molecular simulations have greatly helped in understanding several properties of dendrimers both in solution and in the melt phase.[24−28] In particular, three different molecularly based dendrimer models are commonly employed. The first is the all atom (AA) model, where all the degrees of freedom of the molecule are taken into account, and the chemistry of the dendrimer is completely preserved. With this approach, the behavior of, for example, polyaminoamide (PAMAM) dendrimers in water[29] and bulk[30] has been clarified, predicting their conformational properties and aggregation mechanism. A second simulation approach uses coarse-grained (CG) models to simulate dendrimers. In this case, two different families of CG models are normally employed. One method develops models and force fields from detailed atomistic simulations,[12,31] retaining implicitly the details of the underlying chemistry. Within these models, there is a one-to-one correspondence among the atomistic and CG structure, and the latter is usually built on the former, also providing an easy way to reintroduce in a second stage the degrees of freedom neglected during the coarse-graining procedure.[32,33] The second method uses a simplified CG model where the chemical details are not included.[10,16,34−37] In this case, the potential energy is defined by a bond term that maintains the topology of the molecule and by a nonbonded term to describe all the other pair interactions among beads that are not directly connected. The covalent bonds are usually represented by the attractive finite extensible nonlinear elastic (FENE) potential, where the maximum bond extension can be varied. The nonbonded potential term is usually a shifted Lennard-Jones potential that vanishes at distances beyond a cutoff (r_{cut}). Within this model, several structural properties can be calculated, but the correspondence with the all atom models (and in turn the chemistry of the molecule) is not straightforward as in the previous case. Indeed, each bead corresponds to a Kuhn segment (or persistence length) of the dendron, as the only intrinsic rigidity of the molecule arises from the excluded-volume interactions.

*Corresponding author. E-mail: paola.carbone@manchester.ac.uk.

Published on Web 10/15/2010

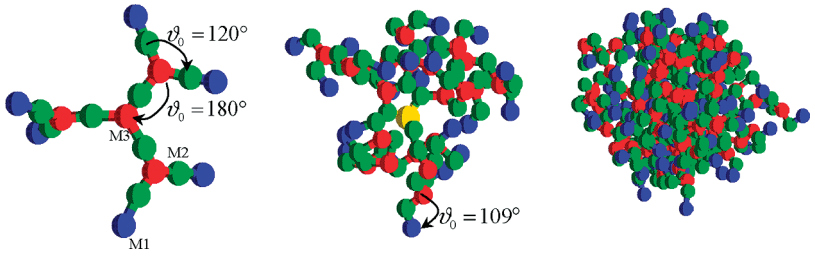

Figure 1. (Left) Snapshot of model_180 second generation dendrimer (d2g2). The equilibrium angles (ϑ_0) are also reported. (Center) Snapshot of model_109 third generation dendrimer (d2g3); the dendrimer core is colored in yellow. (Right) Snapshot of flexible model of the fifth generation dendrimer (d2g5). In the figure, the end-monomers are colored in blue (named M1 in the text), the separator beads are in green (named M2 in the text), and the branching beads are in red (M3 in the text).

However, while for linear polymers the concept of Kuhn length corresponds to a defined distance along the polymer chain (usually measured in bond units) and, from which, the underlying all atomistic structure can be recovered,[38] for dendrimers the Kuhn length is more complicated to define.

Experimentally, due to their constrained topology, dendrimers show a strong correlation among the positions of atoms belonging to the same dendron, and their global structural properties ultimately depend upon the chemistry involved. Gorman et al.[39] used AA models to analyze the effect that the repeat unit flexibility has on the dendrimer conformation. They found that the degree of flexibility of the dendrimer unit affects the global shape of the molecule: dendrimers with a flexible repeat unit possess an eccentric but globular shape, while dendrimers with stiff-chain (phenylacetylene) repeat units are more disk-like in shape. This intimate properties−dendron flexibility relationship can also be found by examining the different behaviors PAMAM[30]and polyphenylene (PD)[31] dendrimers show in bulk phase. The former (flexible dendrimers) shows an evident backfolding of the end-group monomers toward the dendrimer core and clear interpenetration among different molecules, while the latter (typical example of rigid dendrimers) presents a substantially rigid structure that does not allow for backfolding of the end groups. While the intrinsic stiffness of the dendrons comes automatically with the chemistry when AA models (or atomistic-based CG models) are used, for the simplified CG model the intrinsic rigidity of the dendrons can be controlled by including an extra term (bending) to the potential energy.[40]

The present paper aims at predicting the dependence of the dendrimer bulk density upon the dendrimer molecular weight and structure, employing CG models whose dendrons have different degrees of flexibility. In particular, we perform molecular dynamics simulations of simplified CG dendrimers with added local intrinsic stiffness controlled via an additional three-body angular potential. We correlate the value of the bulk density with the amount of free volume of the end-groups, investigating whether, like for linear polymers, the value of bulk density is related to the extra free volume of the chain ends.

Models Employed and Computational Details

We perform molecular dynamics simulations on a melt of CG dendrimers of generation ranging from 1 to 5. Each of the model dendrimers has the same number of beads between the branch points (separator bead, see Figure 1) and are labeled as d2g*n* where n is the generation number while the number "2" indicates the connectivity of the branching beads. In Figure 1, the model for the second (d2g2), third (d2g3), and fifth (d2g5) generation dendrimers are depicted. Beads with different connectivity and position in the dendrimer structure are named differently: the end-dendron beads with one covalent bond are named M1 (colored in blue in Figure 1), separator beads with two covalent bonds are named M2 (colored in green in Figure 1), and finally, the branching beads with three covalent bonds are named M3 (colored in red in Figure 1).

To model the dendrimers, we employ a simplified CG model. Beads that are covalently bonded interact through a harmonic potential U_b

$$U_b(r) = k_b(l - l_0)^2 \tag{1}$$

where r is the distance between the centers of the beads. Beads not directly bonded interact with a Weeks−Chandler−Anderson potential: a truncated, shifted Lennard-Jones potential which is purely repulsive

$$\begin{aligned} U_{\mathrm{WCA}}(r) &= 4\varepsilon\left[\left(\frac{\sigma}{r}\right)^{12} - \left(\frac{\sigma}{r}\right)^{6}\right] + \varepsilon, \quad \text{for } 0 < r < r_{cut} \\ U_{WCA}(r) &= 0, \qquad\qquad\qquad\qquad \text{for } r \geq r_{cut} \end{aligned} \tag{2}$$

To include local rigidity in the dendrimer structure, an additional bond angle potential (U_a) is applied between beads connected by two covalent bonds

$$U_a(r) = k_a(\vartheta - \vartheta_0)^2 \tag{3}$$

The nonbonded WCA interactions are not calculated between the beads interacting through the angular potential.

All the simulation results are reported in LJ reduced units throughout this paper, where the mass m, the potential well depth ε, and the diameter σ of the bead define the unit system for the mass, the energy, and the length, respectively. The cutoff radius applied for the WCA interactions is $r_{cut} = 2^{1/6}\sigma$. The spring constant for the harmonic potential for the bonds is chosen as $k_b l_0^2/K_{\mathrm{B}}T = 0.017$ (where K_{B} is the Boltzmann constant, and T is the absolute temperature) and with $l_0 = 1\sigma$. For the models with the added intrinsic rigidity, we distinguish two cases: one where the equilibrium angle ϑ_0 is set equal to 109° for all angles (this model is named model_109) and a second case where ϑ_0 is set equal to 180° for those angles with the vertex on the branching bead, and $\vartheta_0 = 120°$for all the other angles (this model is named model_180) (see Figure 1). Thus, the first model has an equilibrium angle typical of the flexible aliphatic chains, while the second one resembles the rigid structure of the conjugated polyaromatic dendrimers. In all cases, the harmonic constant for the bending potential is chosen as $k_a\vartheta_0^2/\mathrm{K_B}T = 580$.

Isothermal−isobaric (NPT) MD simulations are performed with the GROMACS molecular dynamics package.[41−43] The temperature and pressure are set to $T = 1.25$ (i.e., $K_{\mathrm{B}}T/\varepsilon = 0.8$) and $P = 3.75$, and a time step of $\Delta t = 0.001$ is used; the simulations are performed for 1 million time steps on a cubic box of 216 first generation dendrimers (d2g1). Since the number of beads increases dramatically upon increasing the dendrimer generation, in order to facilitate the simulations for dendrimers of generations higher than 1, only 125 molecules are used. The temperature is kept constant using the Berendsen thermostat with a coupling

time of 0.1. To maintain a fixed pressure, the Berendsen barostat[44] is employed with a coupling time of 16.605. At this temperature, the WCA potential behaves similarly to a hard sphere system with a diameter of σ.[45] Consequently, the model dendrimers can be considered tangent hard spheres molecules. In order to check that the choice of the constant of the bending potential (k_a) does not affect the results, additional simulations are run with a lower value of k_a ($k_a\vartheta_0^2/K_BT = 290$ with $T = 1.25$). The two set of simulations produce the same results.

The initial configuration of the system is prepared by first initializing a dendrimer in a fully extended conformation, with the separator beads fully stretched and the branch angles at 120°. An energy minimization run is then performed on this isolated dendrimer, followed by a brief molecular dynamics run. The resulting conformation is then replicated and packed into a simple cubic lattice in a sufficiently large cubic box (with periodic boundary conditions) such that they do not overlap. A molecular dynamics simulation run is then performed where the box is slowly compressed to the required density. The simulation box is then re-equilibrated with the full potential ($U_b + U_{LJ}$ or $U_b + U_a + U_{LJ}$ depending if we want to simulate either fully flexible or rigid dendrimers, respectively) using the steepest descendent energy minimization method until the force tolerance is less than $F^* = 10$; in all cases, no more than 1000 energy minimization steps are performed.

For each dendrimer generation we run *NPT* simulations for melts of both the fully flexible and rigid models.

Results

1. Single Molecule Gyration Radius. The conformation of a dendrimer can be characterized through the calculation of the gyration radius R_g which is defined as trace of the gyration tensor ($\mathbf{R}^2$)

$$\mathbf{R}_{\alpha,\beta}{}^2 = \frac{1}{N}\sum_{i=1}^{N}(\mathbf{r}_\alpha^i - \mathbf{r}_\alpha^M)(\mathbf{r}_\beta^i - \mathbf{r}_\beta^M); \quad \alpha,\beta = x,y,z \qquad (4)$$

where N is the number of atoms in the molecule, $\mathbf{r}_\alpha^i$ is the position of the ith atom and $\mathbf{r}_\alpha^M$ is the position of the dendrimer's geometrical center.

$$R_g{}^2 = I_1 = \mathrm{tr}(\mathbf{R}^2) = \lambda_1{}^2 + \lambda_2{}^2 + \lambda_3{}^2 \qquad (5)$$

where $\lambda_1{}^2$, $\lambda_2{}^2$, and $\lambda_3{}^2$ represent the characteristic lengths of the equivalent ellipsoid which describes the dendrimer.

Figure 2 shows how the radius of gyration changes with the number of beads (N) of the dendrimer molecules. Flexible dendrimers follow the scaling law $R_g \approx N^v$, where the scaling exponent $v = 0.330 \pm 0.005$ (linear fitting in Figure 2).[26,46] It is interesting to notice that this scaling law is followed by flexible dendrimers irrespective of which bonding potential is used (harmonic, as in this case, or nonharmonic[16]). On the contrary, the rigid dendrimers deviate from the predicted scaling law. These results highlight the differences between the two rigid models used. The rigid_109 model shows same radius of gyration as the flexible one for generations smaller than three; for higher generations, the R_g values increase more rapidly than that predicted and become more similar to those calculated for the rigid_180 model. The latter, instead, possesses an R_g consistently higher than the flexible model, which cannot be fitted with the exponential scaling law. The degree of asphericity (A) of the dendrimers can be determined from the eigenvalues of the gyration tensor (λ). Indeed, the asphericity (A) of an object is defined as

$$A = \frac{\langle (T_r{}^2 - 3M)\rangle}{\langle T_r{}^2\rangle}$$

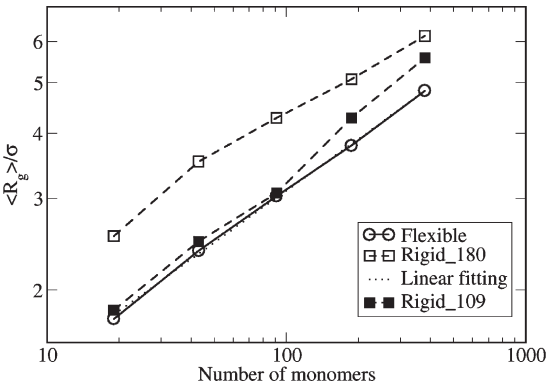

Figure 2. Radius of gyration for the flexible, rigid_109 and rigid_180 dendrimer model.

where $T_r = \lambda_1{}^2 + \lambda_2{}^2 + \lambda_3{}^2$ and $M = \lambda_1{}^2\lambda_2{}^2 + \lambda_2{}^2\lambda_3{}^2 + \lambda_1{}^2\lambda_3{}^2$; A ranges from zero for spherical objects to 1 for extremely elongated objects. We find that all the dendrimer models studied here are nearly spherical, with A ranging between 1×10^{-3} (flexible models) and 4.5×10^{-3} (rigid_180 models). As we will show in the following paragraphs, the main structural difference between the models is indeed the distribution of the monomers within the molecule, rather than their global shape. Flexible dendrimers are characterized by a dense distribution of the beads and reduced internal free volume. On the contrary, the rigid models (the rigid_109 model and in particular the rigid_180 one), due to the introduced intrinsic stiffness, show a larger internal free volume even if they keep a spherical symmetry in their shape. (see Figure 1).

2. Bulk Density and Free Volume. At a fixed temperature, the bulk density (ρ) of a polymer melt depends on its molecular weight (M_w), and according to the free-volume theory,[19] its value can be written as a function of the excess chain-end free volume (V_e) as

$$\rho(T, M_w) = \left[\frac{1}{\rho(T,\infty)} + \frac{2V_e(T)}{M_w}\right]^{-1} \qquad (6)$$

where T is the temperature, $\rho(T,\infty)$ represents the mass density which depends only on the temperature, and V_e is the excess free volume associated with the chain-end. Thus, the second term of eq 6 represents the dependence of the mass density to the chain-end free volume (that in turn depends upon the temperature) existing in addition to the regular contribution of the last monomer. The higher is the molecular weight of the polymer chain the lower is the effect of V_e since it represents a lower fraction of the entire free volume. For polymer melts, the bulk density is expected to increase with M_w up to a specific value (different for different polymers) above which ρ approaches the constant value $\rho(T,\infty)$. Moreover, it has been shown that ρ and V_e depend linearly on temperature (Cohen−Turnbull preposition).[47] Hence, for linear polymers, the variables that affect the bulk density are well established, and the Cohen−Turnbull equation allows the prediction of the value of $\rho(T,\infty)$ and V_e at different temperatures. Experiments[48] and simulations[18] have proven that for linear polymers, the free volume theory is always valid.

It is expected that for dendritic molecules, if the free volume theory can be still applied in the form used for linear polymers, a different function relates the inverse of the density with M_w[7,20] (that throughout this paper means also generation when referred to dendrimers). Indeed, unlike linear polymers, dendrimers have a number of chain-ends (n_e) that varies with M_w (i.e., generation). Thus, for dendrimers, eq 6

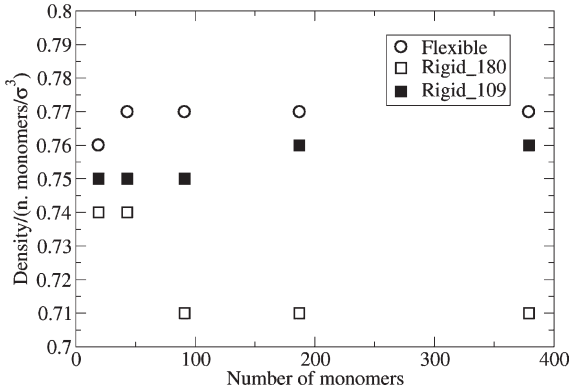

Figure 3. Bulk density as a function of dendrimer molecular weight.

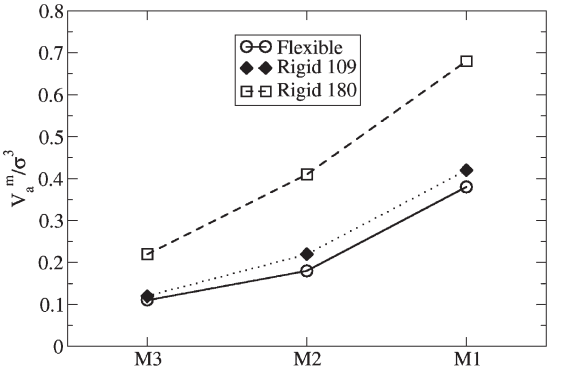

Figure 4. Averaged accessible volume for the three different types of monomers (M1, M2, and M3) for the fifth generation dendrimer (d2g5).

can be rewritten as

$$\rho(T, M_w) = \left[\frac{1}{\rho(T,\infty)} + \frac{n_e(M_w)V_e(T, M_w)}{M_w}\right]^{-1} \quad (7)$$

where both V_e and n_e depend on the M_w. The fact that V_e depends on the M_w is a hypothesis at this stage and must be verified.

Figure 3 shows the density of flexible and rigid dendrimers as a function of their molecular weight (number of monomers). From the figure, it is clear that dendrimers show a different trend of their bulk density compared with linear polymers. For the flexible dendrimers, ρ is constant for generations larger than two and slightly increases moving from generation one to generation two. It is also clear that the intrinsic rigidity of the dendrons themselves does not affect the value of density. The two systems with intrinsic rigidity but different equilibrium angles (rigid_109 and rigid_180 in the figure) are characterized by different trends in their ρ. Dendrimers with an equilibrium angle equal to 109° show densities very similar to those of the flexible dendrimers of same generation (except a small difference for generation two and three). On the contrary, the models with an equilibrium angle set to 180° (only among monomers connecting the generation, see Figure 1) show a dramatic decrease in the bulk density for generations larger than two.

As n_e and, probably, V_e of eq 7 depend on the M_w, the only way to get an estimate of the excess free volume of the end monomers (V_e) is then to carry out its direct calculation from the simulations. Following ref 18, V_e can be interpreted as the extra accessible free volume associated with the end-monomers, in addition to that generated near any other monomers in the molecule. The accessible free volume (V_a) represents the volume of the space accessible to a spherical probe of specific radius created by rolling it over the van der Waals molecule surface (the surface of the union of the spherical atomic surfaces defined by their van der Waals radius). We compute V_a performing a free volume analysis using the method developed by Connolly and Richards[49,50] with a probe of radius equal to the size of the monomers.

Figure 4 shows the values of the mean accessible volume for the three different types of monomers (M1, M2, and M3) averaged on all the monomers of the same type (V_a^m). In the figure, only the values obtained for the flexible and rigid models of the d2g5 dendrimer are compared, but similar behavior is exhibited by all the other dendrimers investigated here. From the figure, it appears clear that there is a hierarchical distribution of the accessible volume among monomers of different types. The V_a^m of the end-monomers (type M1) is larger compared to that associated with the internal ones M2 and M3, and the latter has, in turn, a smaller V_a^m than M2. Thus, unlike in polymers where the internal monomers have an evenly distributed V_a^m and only the chain-end monomers, or other few directly attached to them along the chain, show a different (higher) V_a^m,[18] in dendrimers, due to their constrained topology, the V_a^m is distributed differently between the monomers depending upon their connectivity and position within the dendrons. Monomers with three bonds (M3) show the smallest V_a^m, and their values are almost identical in the flexible and rigid_109 models. In the rigid_180 model, the M3 monomer has as well the smallest associated V_a^m, but its value is comparable with that of the M2 monomer of the flexible and even rigid_109 dendrimer. The high V_a^m values found for the rigid_180 model show that there is free volume retained within the molecular scaffold and that this volume is larger in this model than in the others investigated here. These results explain the similar bulk density values obtained for the flexible and rigid_109 models, but they do not justify the flat distribution of the ρ values obtained for dendrimers of the same type (rigid or flexible) but of different generations. To understand this peculiar behavior, one has to remember that in dendrimers the number of monomers increases with the M_w (i.e., generations), and n_e in eq 7 is indeed dependent on M_w.

In Figure 5, the overall contribution (V_a^{mol}) of monomers of type m to the total access free volume of the dendrimer, normalized by M_w, is reported for the different monomer types as a function of the dendrimer generation. V_a^{mol} is defined as

$$V_a^{mol}(M_w, m) = \frac{1}{M_w}\sum_{i=1}^{N_m} V_a^m(M_w, i) \quad (8)$$

where the sum runs over the N_m distinct types of monomers (m = M1, M2, or M3), M_w is the molecular weight of the dendrimer molecule, and $V_a^m(M_w,i)$ is the accessible free volume of a specific monomer i of type m, whose value depends upon the generation of the dendrimer (M_w). In Figure 5, V_a^{mol} is reported for all the monomer types and not only for the end-chain ones (M1). These results highlight the difference between the linear polymer and the dendrimer cases. For linear polymers the total accessible volume of the internal monomers increases with M_w (as the number of internal monomers increase), while the value of the accessible free volume associated with the two end-chain monomers should not change with the degree of polymerization.[18] On the contrary here, since the number of monomer types (N_m) follows the order $N_{M2} > N_{M1} > N_{M3}$, it happens that the total accessible volume associated with the end-monomers (M1) and that associated with the monomers with two connections

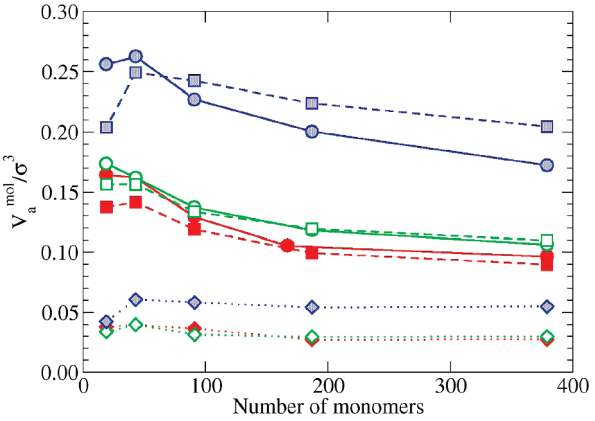

Figure 5. Accessible volume per molecule of dendrimer calculated for the different beads M1 (circle), M2 (square), and M3 (diamond) of the flexible (in red solid symbols), rigid_109 (in green open symbols), and rigid_180 (in blue shaded symbols) models. Lines are drawn to guide the eye.

(M2) have just about the same value, and, for generations larger than three, this value becomes almost constant. Moreover, for the rigid dendrimer with a linear spacer (rigid_180), $V_a^{mol}(M_w, M2)$ is even larger than the corresponding value of the end-monomers (i.e., $V_a^{mol}(M_w,M1)$. It should be noted, however, that the definition of V_e in eq 7 differs from that of $V_a^m(M1)$ (i.e., the accessible volume of the end-monomer M1 of eq 8). Indeed, V_e represents the extra accessible volume associated with the chain ends in addition to that generated near any other internal monomers. For linear polymers, Harmandaris et al.[18] noted that V_e and V_a of the chain ends show the same trend with the temperature; thus, V_a is a qualitative reference to investigate the change of V_e with the temperature. Moreover, V_e can be easily calculated from the V_a of the chain ends by subtracting the V_a of the internal monomers from it.[18] In the present case, it is difficult to say if only the free volume associated with the M1 monomers should be included in the calculation of the V_e since V_a is equally distributed between M1 and M2. In any case, from Figure 5 it appears clear that either if $V_a^m(M2)$ is included or not in the calculation of V_e, the ratio $n_e(M_w)V_e(T,M_w)/M_w$ of eq 7 (at the temperature simulated here) is almost constant for generations higher than three in all the models investigated and this justifies the constant bulk density observed.

It is interesting to notice that our computational findings agree and rationalize experimental and simulation data available in the literature, such as the weak dependency of bulk density and the glass transition temperature with the dendrimer generation found for flexible dendrimers (like PAMAM or PPI) with different end-group functionalities or the bulk density rigid polyphenilene dendrimers.[7,20,30,31,51]

3. Interdendrimer Packing. The low free volume associated with the internal monomers of the flexible models is due to their well-known collapsed conformation with a pronounced backfolding of the dendrons toward the dendrimer core.[36,52] This is clear from Figure 6 where the intradendrimer radial distribution function (RDF) for the d2g2 flexible and rigid_180 model is reported. Indeed, even at small generations the bend of the arms toward the dendrimer core is visible for the fully flexible model. As can be seen from the radius of gyration, the use of a nonharmonic potential as the FENE does not affect the intramolecular distribution, which compares well with previous simulation results.[16] In contrast for the rigid_180 dendrimers, the presence of an extra bending potential favors the elongation of the dendrons toward the outer part of the molecule. However, it is worth noticing that the enhanced local rigidity does not affect the global shape of the dendrimer

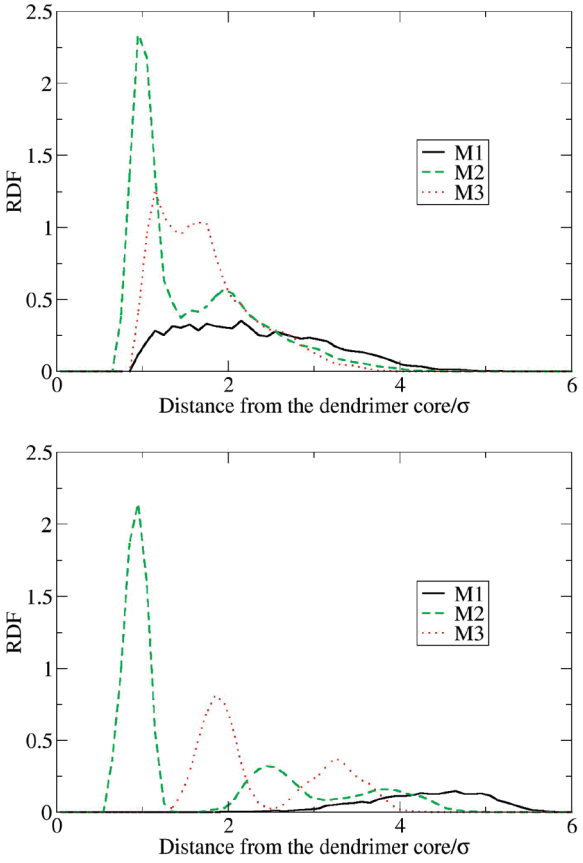

Figure 6. Intradendrimer radial distribution function with respect to the distance from the dendrimer core for the d2g2 flexible (upper panel) and d2g2 rigid_180 (lower panel) model.

that (as mentioned in part 1 of this section) remains spherical on average. In the rigid_180 models, the regular organization of the arms (see Figure 1) leaves quite a lot empty volume among them, making easier the interpenetration among the dendrimers even at high generation.

The effect of the interdendrimer packing can be seen from the total (inter and intra dendrimers) radial distribution function (shown in Figure 7). The added stiffness of the dendrons affects the short-range order, as has been observed for the case of linear polymers.[53] The first peak of the RDF of Figure 7 is indeed lower for the rigid models than for the flexible one. The flexible dendrimer shows also a clear second peak of lower intensity at ca. 2σ. In the rigid models, this second peak broadens and is shifted to a higher distance. The loss of a locally ordered structure is more evident in the rigid_180 models than in the rigid_109 regardless the dendrimer generation, and it is also reflected in the values of the packing fraction $\varphi = \pi N\sigma^3/6V$ (where N is the total number of monomers, and V is the total volume of the system) that are 0.372, 0.398, and 0.40 for the rigid_180, rigid_109, and flexible models, respectively (for generations higher than three). As the rigid_180 model shows a well structured intradendrimer monomer−monomer RDF (see Figure 6 lower panel for the second generation), it is reasonable to assume that the interactions that perturb the local order have an interdendrimer origin. Figure 8 shows the center of mass interdendrimer RDF calculated for selected models. The added rigidity of the dendrons clearly favors the interpenetration of the models. The fully flexible models show for all the generations studied here a soft interaction among their core, as found in previous computational works.[35,54]

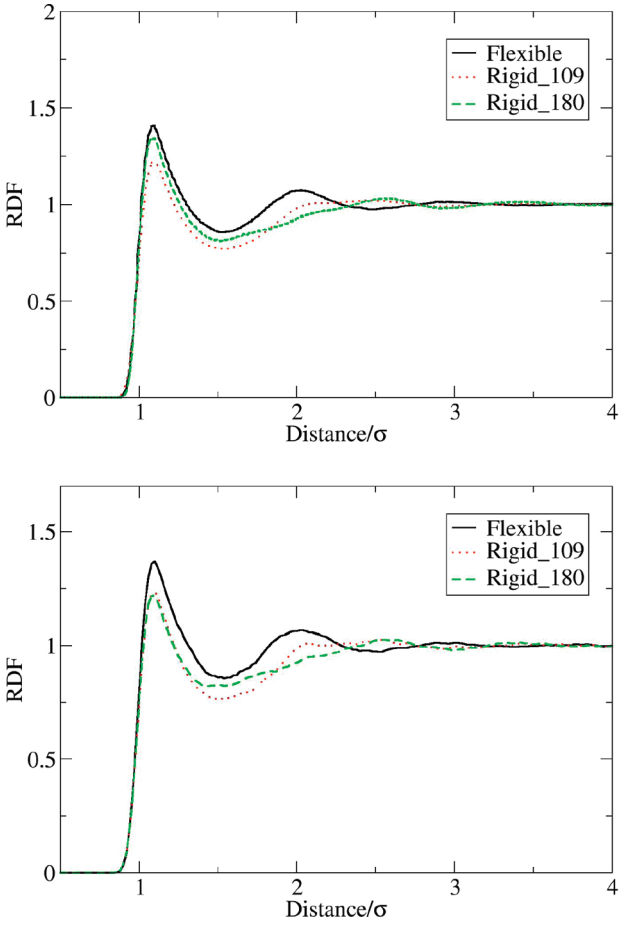

Figure 7. Total radial distribution function of the d2g2 model (upper panel) and the d2g4 model (lower panel).

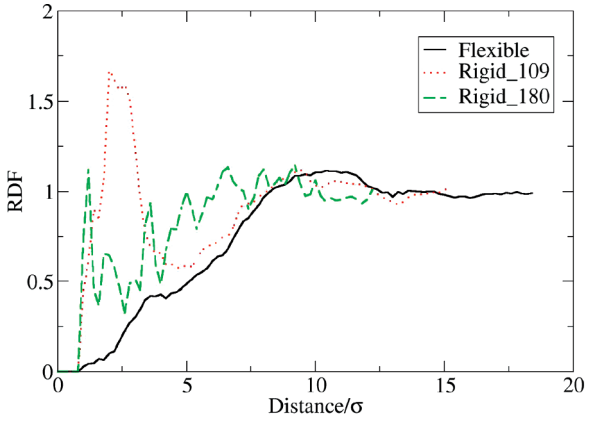

Figure 8. Center of mass interdendrimer radial distribution function for d2g5 flexible model (solid black line), d2g4 rigid_109 model (dotted red line), and d2g3 rigid_180 model (dashed green line).

On the contrary, the rigid models, except that of the smallest generation (not shown), are characterized by pronounced dendrimer interpenetration, which is evident from the second generation upward for the rigid_180 model and from the third upward for the rigid_109 model.

Summary and Conclusions

By means of molecular dynamics simulations, we calculated the bulk density of model dendrimers characterized by different intrinsic rigidity and molecular weight (i.e., generation). The stiffness was introduced and varied in a systematic way by adding an extra three-body harmonic potential between beads connected by two covalent bonds.

We found that the rigidity affects the dendrimers' radius of gyration, which deviate from the typical scaling law $R_g \approx N^{0.33}$ predicted for flexible models. Small generation dendrimers (smaller than or equal to three) with not fully extended arms (rigid_109 model) show R_gs similar to those observed in the flexible models of the same generations. For generations larger than three the stiffness of the dendrons starts to play a role and a remarkably increase in the R_g values is observed. On the contrary, the rigid models with fully extended arms (rigid_180 models) show a radius of gyration that increases with the model molecular weight deviating, even for small generations, from the predicted scaling law.

We observed that the dependence of the bulk density with the dendrimer molecular weight remarkably differs from what happens in the linear polymer case. In fact the density changes between the first smaller dendrimer generations and then reaches a plateau instead of following the hyperbolic function of the molecular weight typical of linear polymers. We interpreted this peculiar trend of the bulk density in terms of free volume. Computing directly from the simulations the accessible free volume of the different monomers, we showed that unlike linear polymers, in dendrimers the accessible free volume is shared unevenly between the monomers. Moreover, even though the end-dendron monomers are characterized by a higher accessible volume compared to the internal ones, this extra volume is compensated by the lower number of these types of monomers, compared with the internal ones. The final balance leads to an amount of V_a that is almost constant changing the dendrimer generation and, in turn, to the weak dependency of the bulk density with the dendrimer molecular weight. This finding explains and is in agreement with experimental and atomistic simulation data that showed a very mild (if not absent) change in the dendrimer glass transition temperature and density with the change in the dendrimer generation.

The enhanced stiffness of the dendrons does not affect the global shape of the model that keeps the spherical shape that characterizes the fully flexible one. On the contrary, the dendron rigidity changes the short-range order decreasing the local order and the packing efficiency due to an evident dendrimer interpenetration that appears even at the lowest generation.

References and Notes

(1) Tomalia, D. A.; Frechet, J. M. *Prog. Polym. Sci.* **2005**, *30* (3−4), 217–219.
(2) Hay, G.; Mackay, M. E.; Hawker, C. J. *J. Polym. Sci., Part B: Polym. Phys.* **2001**, *39* (15), 1766–1777.
(3) Tomalia, D. A. *Prog. Polym. Sci.* **2005**, *30* (3−4), 294–324.
(4) Gunning, J. P.; Levell, J. W.; Wyatt, M. F.; Burn, P. L.; Robertson, J.; Samuel, I. D. W. *Polym. Chem.* **2010**, *1* (5), 730–738.
(5) Caminade, A.-M.; Majoral, J.-P. *Acc. Chem. Res.* **2004**, *37* (6), 341–348.
(6) Schlupp, M.; Weil, T.; Berresheim, A. J.; Wiesler, U. M.; Bargon, J.; Müllen, K. *Angew. Chem., Int. Ed.* **2001**, *40* (21), 4011.
(7) Wooley, K. L.; Hawker, C. J.; Pochan, J. M.; Frechet, J. M. J. *Macromolecules* **1993**, *26* (7), 1514–1519.
(8) Farrington, P. J.; Hawker, C. J.; Frechet, J. M. J.; Mackay, M. E. *Macromolecules* **1998**, *31* (15), 5043–5050.
(9) Le, T. C.; Todd, B. D.; Daivis, P. J.; Uhlherr, A. *J. Chem. Phys.* **2009**, *131* (4), 044902.
(10) Bosko, J. T.; Prakash, J. R. *J. Chem. Phys.* **2008**, *128* (3), 034902.
(11) Le, T. C.; Todd, B. D.; Daivis, P. J.; Uhlherr, A. *J. Chem. Phys.* **2009**, *130* (7), 074901.
(12) Lee, C. K.; Hua, C. C.; Chen, S. A. *J. Phys. Chem. B* **2009**, *113* (49), 15937–15948.
(13) Lue, L. *Macromolecules* **2000**, *33* (6), 2266–2272.
(14) Lue, L.; Prausnitz, J. M. *Macromolecules* **1997**, *30* (21), 6650–6657.
(15) Vicinelli, V.; Ceroni, P.; Maestri, M.; Lazzari, M.; Balzani, V.; Lee, S. K.; van Heyst, J.; Vogtle, F. *Org. Biomol. Chem.* **2004**, *2* (15), 2207–2213.

(16) Bosko, J. T.; Todd, B. D.; Sadus, R. J. *J. Chem. Phys.* **2004**, *121* (2), 1091–1096.
(17) Rathgeber, S.; Monkenbusch, M.; Kreitschmann, M.; Urban, V.; Brulet, A. *J. Chem. Phys.* **2002**, *117* (8), 4047.
(18) Harmandaris, V. A.; Doxastakis, M.; Mavrantzas, V. G.; Theodorou, D. N. *J. Chem. Phys.* **2002**, *116* (1), 436–446.
(19) von Meerwall, E.; Beckman, S.; Jang, J.; Mattice, W. L. *J. Chem. Phys.* **1998**, *108* (10), 4299–4304.
(20) Morgan, D. R.; Stejskal, E. O.; Andrady, A. L. *Macromolecules* **2000**, *32*, 1897–1903.
(21) Zook, T. C.; Pickett, G. T. *Phys. Rev. Lett.* **2003**, *90* (1), 015502.
(22) Carbone, P.; Calabretta, A.; Di Stefano, M.; Negri, F.; Müllen, K. *J. Phys. Chem. A* **2006**, *110* (6), 2214–2224.
(23) Carbone, P.; Rapallo, A.; Ragazzi, M.; Tritto, I.; Ferro, D. R. *Macromol. Theory Simul.* **2006**, *15* (6), 457–468.
(24) Karatasos, K. *Macromolecules* **2005**, *38* (10), 4472–4483.
(25) Karatasos, K. *Macromolecules* **2006**, *39* (13), 4619–4626.
(26) Murat, M.; Grest, G. S. *Macromolecules* **1996**, *29* (4), 1278–1285.
(27) Terao, T. *Chem. Phys. Lett.* **2007**, *446* (4−6), 350–353.
(28) Ballauff, M.; Likos, C. N. *Angew. Chem., Int. Ed.* **2004**, *43* (23), 2998–3020.
(29) Maiti, P. K.; Cagin, T.; Lin, S. T.; Goddard, W. A. *Macromolecules* **2005**, *38* (3), 979–991.
(30) Carbone, P.; Müller-Plathe, F. *Soft Matter* **2009**, *5* (13), 2638–2647.
(31) Carbone, P.; Negri, F.; Müller-Plathe, F. *Macromolecules* **2007**, *40* (19), 7044–7055.
(32) Karimi-Varzaneh, H. A.; Carbone, P.; Müller-Plathe, F. *J. Chem. Phys.* **2008**, *129* (15), 154904.
(33) Chen, X. Y.; Carbone, P.; Santangelo, G.; Di Matteo, A.; Milano, G.; Müller-Plathe, F. *Phys. Chem. Chem. Phys.* **2009**, *11* (12), 1977–1988.
(34) Ganazzoli, F.; La Ferla, R.; Raffaini, G. *Macromolecules* **2001**, *34* (12), 4222–4228.
(35) Harreis, H. M.; Likos, C. N.; Ballauff, M. *J. Chem. Phys.* **2003**, *118* (4), 1979–1988.
(36) Gotze, I. O.; Likos, C. N. *J. Phys.: Condens. Matter* **2005**, *17* (20), S1777–S1797.
(37) Mladek, B. M.; Kahl, G.; Likos, C. N. *Phys. Rev. Lett.* **2008**, *100* (2), 154904.
(38) Carbone, P.; Karimi-Varzaneh, H. A.; Müller-Plathe, F. *Faraday Discuss.* **2010**, *144*, 25–42.
(39) Gorman, C. B.; Smith, J. C. *Polymer* **2000**, *41* (2), 675–683.
(40) Bulacu, M.; van der Giessen, E. *J. Chem. Phys.* **2005**, *123* (11), 114901.
(41) Berendsen, H. J. C.; van der Spoel, D.; van Drunen, R. *Comput. Phys. Commun.* **1995**, No. 91, 43–56.
(42) Lindahl, E.; Hess, B.; van der Spoel, D. *J. Mol. Model.* **2001**, *7* (8), 306–317.
(43) Van der Spoel, D.; Lindahl, E.; Hess, B.; Groenhof, G.; Mark, A. E.; Berendsen, H. J. C. *J. Comput. Chem.* **2005**, *26* (16), 1701–1718.
(44) Berendsen, H. J. C.; Postma, J. P. M.; van Gusteren, W. F.; Di Nola, A.; Haak, J. R. *J. Chem. Phys.* **1984**, *81* (8), 3684–3690.
(45) Gao, J.; Weiner, J. H. *J. Chem. Phys.* **1989**, *91* (5), 3168–3173.
(46) Giupponi, G.; Buzza, D. M. A. *J. Chem. Phys.* **2004**, *120* (21), 10290–10298.
(47) Cohen, M. H.; Turnbull, D. *J. Chem. Phys.* **1959**, *31* (5), 1164–1169.
(48) Dlubek, G.; Sen Gupta, A.; Pionteck, J.; Krause-Rehberg, R.; Kaspar, H.; Lochhaas, K. H. *Macromolecules* **2004**, *37* (17), 6606–6618.
(49) Connolly, M. L. *J. Appl. Crystallogr.* **1983**, *16*, (OCT), 548−558.
(50) Connolly, M. L. *J. Am. Chem. Soc.* **1985**, *107* (5), 1118–1124.
(51) Tande, B. M.; Wagner, N. J.; Kim, Y. H. *Macromolecules* **2003**, *36* (12), 4619–4623.
(52) Rosenfeldt, S.; Dingenouts, N.; Ballauff, M.; Werner, N.; Vogtle, F.; Lindner, P. *Macromolecules* **2002**, *35* (21), 8098–8105.
(53) Faller, R.; Kolb, A.; Müller-Plathe, F. *Phys. Chem. Chem. Phys.* **1999**, *1* (9), 2071–2076.
(54) Gotze, I. O.; Harreis, H. M.; Likos, C. N. *J. Chem. Phys.* **2004**, *120* (16), 7761–7771.